Damage threshold investigation using grazing incidence irradiation by hard X-ray free electron laser

T. Koyama[a], H. Yumoto[a], K. Tono[a], T. Sato[b], T. Togashi[a], Y. Inubushi[b], T. Katayama[a], J. Kim[c], S. Matsuyama[c], H. Mimura[d], M. Yabashi[b], K. Yamauchi[c], H. Ohashi[a]

[a]Japan Synchrotron Radiation Research Institute (JASRI), 1-1-1 Kouto, Sayo-cho, Sayo-gun, Hyogo 679-5198, Japan

[b]RIKEN SPring-8 center, 1-1-1 Kouto, Sayo-cho, Sayo-gun, Hyogo 679-5148, Japan

[c]Department of Precision Science & Technology, Graduate School of Engineering, Osaka University, 2-1 Yamadaoka, Suita, Osaka 565-0871, Japan

[d]Department of Precision Engineering, Graduate School of Engineering, The University of Tokyo, 7-3-1, Hongo, Bunkyo-ku, Tokyo 113-8656, Japan

ABSTRACT

X-ray free electron lasers (XFELs) with intense and ultra-short pulse X-rays possibly induce damage to optical elements. We investigated the damage thresholds of optical materials by using focusing XFEL beams with sufficient power density for studying ablation phenomena. 1-µm focusing beams with 10 keV photon energy were produced at the XFEL facility SACLA (SPring-8 Angstrom Compact free electron LAser). The focusing beams irradiated samples of rhodium-coated substrate, which is used in X-ray mirror optics, under grazing incident condition.

Keywords: X-ray free electron laser, Focusing mirror, Ablation, Damage threshold, Hard X-ray

1. INTRODUCTION

Since the advent of X-ray free electron laser (XFEL) facilities, such as the Linac Coherent Light Source [1] and SPring-8 Angstrom Compact free electron LAser (SACLA) [2], fully transverse coherent X-rays with intense ultra-shot pulse have been available even in the hard X-ray region. Such intense X-rays possibly induce damage to optical elements, which can cause the serious problem of beam quality degradation.

To investigate the damage thresholds of optical elements such as X-ray mirrors, we used focusing XFEL beams with sufficient power density for studying ablation phenomena. Multiple focusing XFEL beams were irradiated to test samples under grazing incident condition.

Low-Z materials such as carbon are often used for coating material. However, the resulting critical angle is small for the hard X-ray region; a metal coating mirror is necessary under large grazing incident angles. We chose rhodium for the coating material of the test sample. This material is widely used in synchrotron beamline mirrors.

The damage thresholds were evaluated by measuring the X-ray reflectivity variation. We report on the results of the experiments.

* koyama@spring8.or.jp; phone +81-791-58-0831; fax +81-791-58-0830

Advances in X-Ray/EUV Optics and Components VIII, edited by Ali Khounsary, Shunji Goto, Christian Morawe, Proc. of SPIE Vol. 8848, 88480T · © 2013 SPIE
CCC code: 0277-786X/13/$18 · doi: 10.1117/12.2025377

2. EXPERIMENTAL SETUP

The experiment was performed at beamline 3 (BL3) of SACLA [2,3]. The SACLA was operated with mean pulse energy of 240 μJ, pulse duration of 20 fs [4], and operation frequency of 10 Hz during the experiment. We chose an X-ray photon energy of 10 keV. A double plane mirror system under grazing incidence angle of 2 mrad was used to reduce higher order harmonics.

The XFEL light was focused down to a diameter of 1 μm (FWHM) using a focusing mirror system [5] consisting of two elliptical mirrors in a Kirkpatrick-Baez configuration. A knife-edge scanning method was used to measure the profile of the focused beam.

An irradiation chamber was designed and installed at the focal point of the focusing mirror system, as shown in Figure 1. This chamber had been tested to investigate the damage thresholds of some optical materials under normal incident condition [6]. The samples were mounted on high-precision stages with a motion range of 50 mm in the vertical and horizontal directions along the optical axis and 15 mm perpendicular to the optical axis. A rotation stage with motion range from -10° to +100° was used to adjust the incident angle. An eccentricity of rotation was adjusted within 30 μm around the angle range of 90°. The surface of the samples was monitored by long working distance optical microscopes at an angle of 30° in the beam profile measurement and 90° in the test sample measurement, as shown in Figures 1 and 2.

Irradiation pulse numbers were 100, 1000 and/or 10000 shots, controlled using a pulse selector [7]. Irradiation pulse energies were controlled using a silicon solid attenuator with various thicknesses. The shot-to-shot fluctuations of the pulse energy were monitored by a scattering-based beam intensity monitor [8]. The maximum deliverable pulse energy to the test sample was 100 μJ, taking into account the air path for inserting the intensity monitor and the attenuator, as well as polyimide and beryllium isolation windows.

Two detectors were used to measure reflected beam intensity. One of these was a scattering-based beam intensity monitor (gas monitor) used for high intensity (> 0.5 μJ), and the other was a PIN photodiode used for low intensity (< 0.5 μJ). A four-quadrant slit, a gas monitor, and a PIN photodiode were mounted on a single optical rail. Two motorized translation stages were used to align the rail position along the reflected beam axis from the sample and to enable a θ-2θ scan with the sample rotation stage. An alignment CCD camera was used to make parallel the focused beam axis and the sample surface.

We chose a rhodium-coated silicon substrate, widely used as an X-ray mirror, for a test sample. The rhodium coating layer was deposited by DC magnetron sputtering. Its thickness was 100 nm, and a 5-nm-thick chromium was inserted as an adhesive layer. The substrate was 50 mm long, 10 mm wide, and 0.5 mm thick.

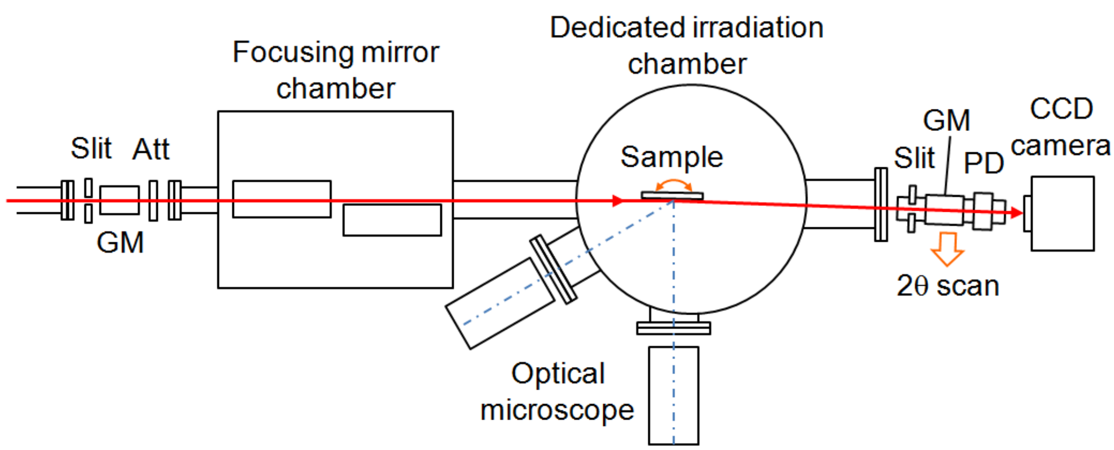

Figure 1. Schematic of experimental setup. GM: Gas monitor, Att: Attenuator, PD: PIN photodiode.

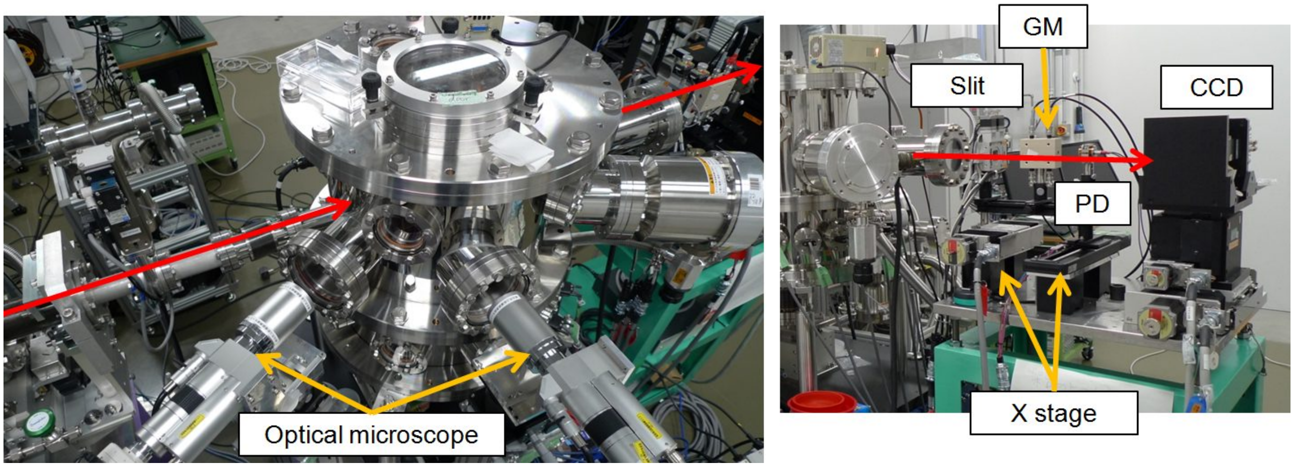

Figure 2. Photographs of the experimental chamber (left) and the detector assembly (right).

3. RESULTS

To precisely determine the incident angle, reflectivity was measured using θ-2θ scanning, as shown in Figure 3. During the measurement, the pulse energy was reduced sufficiently by using a 1500 µm thick silicon attenuator to avoid irradiation damage. The transmittance was 1.3×10^{-5}. In Figure 3, the solid line indicates a simulation with rhodium density of 12.4 g/cm^3 and roughness of 0.8 nm rms. We chose incident angles of 3.74, 5.52, and 6.70 mrad (the critical angle of rhodium) with an angular tolerance better than 0.05 mrad. The reflectivity for the three incident angles were 93%, 84%, and 50%, respectively.

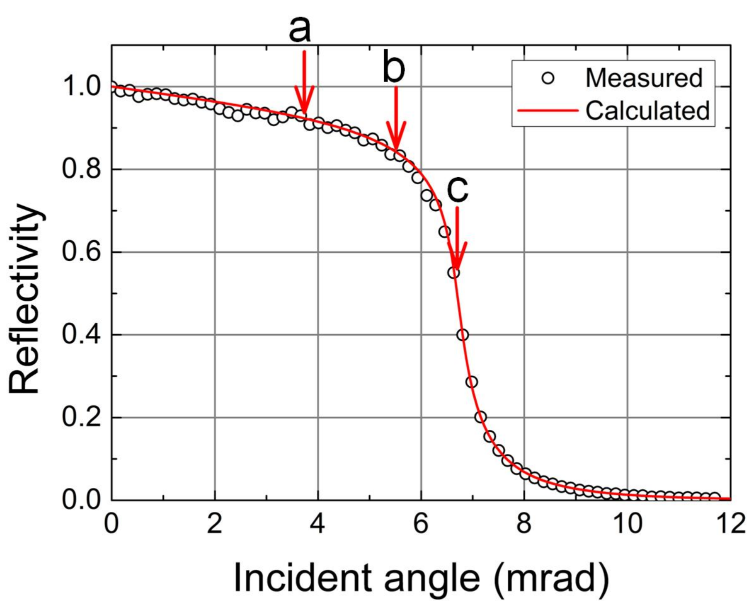

Figure 3. Result of θ-2θ scanning reflectivity measurement. Damage threshold measurements were performed at fixed angles of 3.74 (a), 5.52 (b), and 6.70 mrad (c).

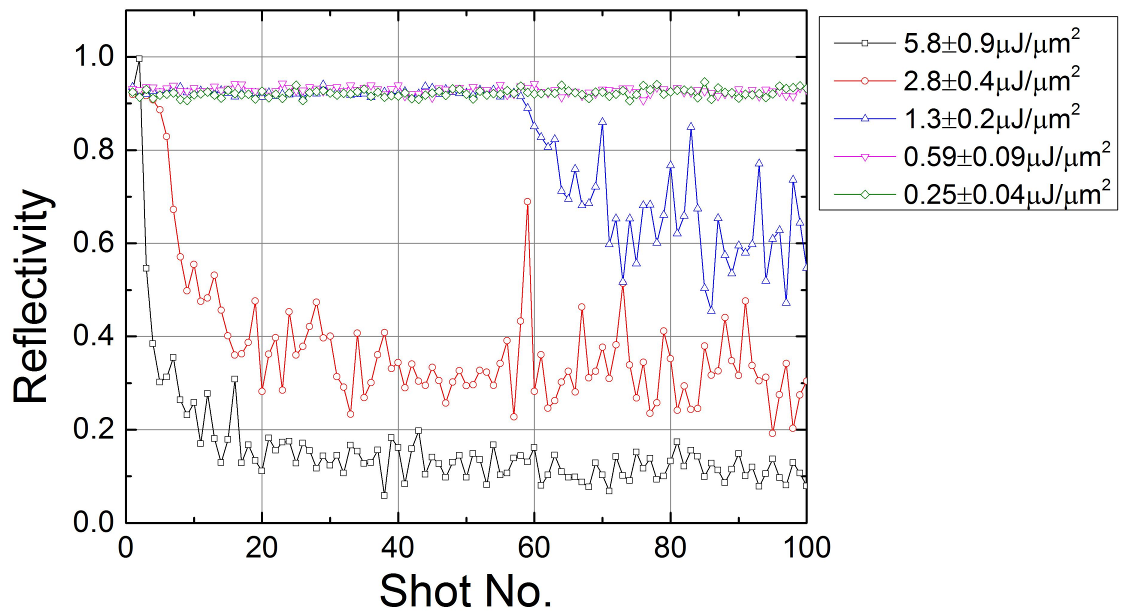

Figure 4. Typical reflectivity variations plotted against shot number. The incident angle is 3.74 mrad.

Figure 4 shows typical reflectivity variations plotted against shot number with various incident fluences. The incident angle is 3.74 mrad, and 100 shots were irradiated. The shot-to-shot reflectivity was monitored during irradiation. Damage could occur at the point of reflectivity change. With fluences of 5.8 $\mu J/\mu m^2$ and 2.8 $\mu J/\mu m^2$, the reflectivity dropped shortly after the irradiation started. With fluence of 1.3 $\mu J/\mu m^2$, the reflectivity dropped after 58 pulses of irradiation. No reflectivity changes were observed with lower fluences. Furthermore, as incident fluence was higher, reflectivity after the damage was lower. Severe damage occurred with high fluences.

Figure 5 shows damaged shot numbers plotted as a function of fluence at several incident angles. Open circles indicate that no damage was observed in shot number 100, 1000, or 10000. Open triangles indicate that damage was observed. The reflectivity changed shot number was plotted. Damage fluences were determined by the intermediate value between the damaged and the survived fluence.

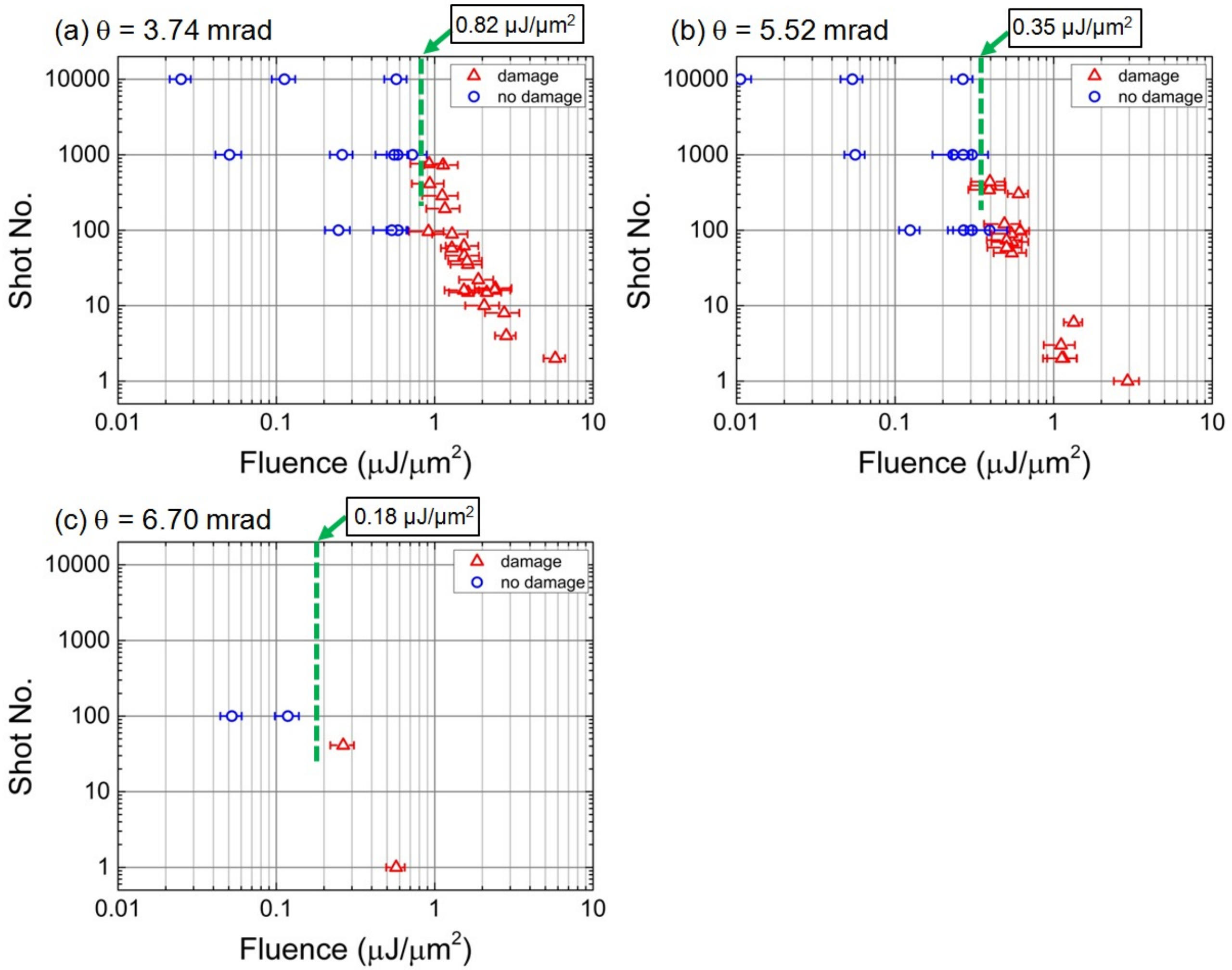

Figure 5. Damaged shot number plotted as function of fluence. (a) Incident angle was 3.74 mrad, reflectivity was 93%. (b) Incident angle was 5.52 mrad, reflectivity was 84%. (c) Incident angle was 6.70 mrad (critical angle), reflectivity was 50%.

Figure 6 shows damage fluence as a function of incident angle. Three obtained damage fluences are plotted. The damage fluences decreased as the incident angle increased. The damage fluence under the normal incidence condition was reported as 0.072 μJ/μm^2 [6]. This value was converted to the dose D_{th} for a single atom to be 0.79 eV/atom. We calculated the fluence F_{th} required for this dose as [9-11]

$$F_{th} = \frac{D_{th} \rho N_A d}{A(1-R)\sin\theta}, \qquad (1)$$

where ρ, N_A, A, R, and θ are the density, Avogadro's constant, the atomic weight, the reflectivity, and the incident angle, respectively. The variable d is the energy deposition depth, given by $d = \sqrt{d_x^2 + d_e^2}$, where d_x is the X-ray penetration depth calculated with the absorption coefficient $\mu_g(\theta)$ as

$$\frac{1}{d_x} = \mu_g(\theta) = \frac{2\sqrt{2}\pi}{\lambda}\sqrt{\sqrt{(2\delta-\theta^2)^2 + 4\beta^2} + 2\delta - \theta^2}\ , \qquad (2)$$

with the complex refractive index $n = 1-\delta+i\beta$, and X-ray wavelength λ. The variable d_e is the electron collisional range [12]. In this case, d_e was assumed to be 30 nm. For comparison, fluence F_{th} without the electron range is shown by the dashed line in Figure 6. The fluence at the critical angle was one order of magnitude smaller than the threshold level considering the electron range. For causing damage to the sample, electron transport seems to be more effective below the critical angle.

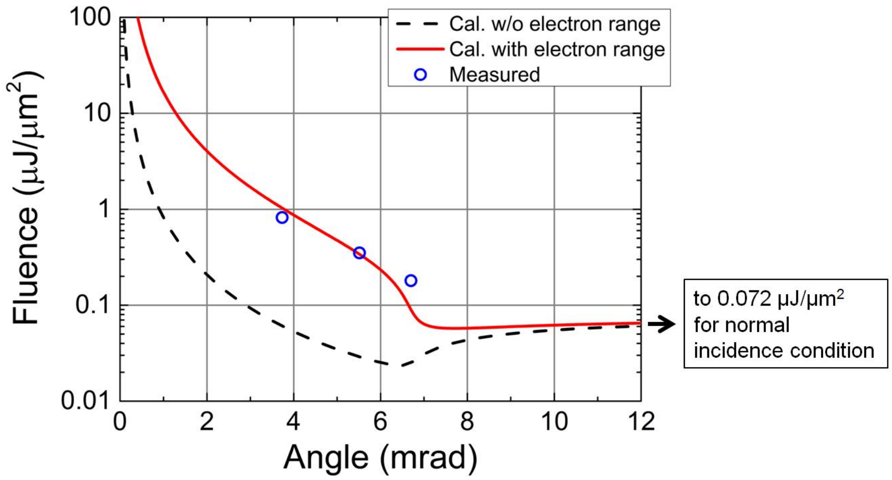

Figure 6. Damage fluence plotted as function of incident angle.

For the practical case at SACLA, the fluence of the direct beam with size of 200 μmϕ (FWHM) and peak pulse energy of 400 μJ at 10 keV is on the order of 0.01 $\mu J/\mu m^2$. This value is 1-2 orders of magnitude lower than the threshold level. Therefore, a metal coating of rhodium is suitable for use below the critical angle.

4. CONCLUSION

We have performed damage measurement of a metal coating test sample under grazing incident condition at the XFEL facility SACLA. The coating material was rhodium. A 1-μm focusing beam with photon energy of 10 keV was used. At grazing incidence angles of 3.74, 5.52, and 6.70 mrad, measured damage fluences were 0.82, 0.35, and 0.18 $\mu J/\mu m^2$, respectively. These values are sufficiently high compared with the fluence of the direct beam at SACLA.

ACKNOWLEDGMENTS

The authors would like to sincerely thank Takanori Miura for his support in measuring the samples, as well as Hikaru Kishimoto and the SACLA engineering team for their help during the beam time. This work was performed at the BL3 of SACLA with the approval of the Japan Synchrotron Radiation Research Institute (JASRI) (Proposal No. 2012B8052). This research was partially supported by a Grant-in-Aid for Scientific Research (S) (23226004) from the Ministry of Education, Sports, Culture, Science and Technology, Japan (MEXT).

REFERENCES

[1] Emma, P. et al., "First lasing and operation of an ångstrom-wavelength free-electron laser," Nature Photon. 4, 641–647 (2010).

[2] Ishikawa, T. et al., "A compact X-ray free-electron laser emitting in the sub-ångstrom region," Nature Photon. 6, 540–544 (2012).

[3] Tono, K., Inubushi, Y., Sato, T., Togashi, T., Ohashi, H., Kimura, H., Takahashi, S., Takeshita, K., Tomizawa, H., Goto, S., and Yabashi, M., "Beamline for X-ray Free Electron Laser of SACLA," J. Phys. Conference Series 425, 072006 (2013).

[4] Inubushi, Y., Tono, K., Togashi, T., Sato, T., Hatsui, T., Kameshima, T., Togawa, K., Hara, T., Tanaka, T., Tanaka, H., Ishikawa, T., and Yabashi, M., "Determination of the pulse duration of an X-ray free electron laser using highly resolved single-shot spectra," Phys. Rev. Lett. 109, 144801 (2012).

[5] Yumoto, H., Mimura, H., Koyama, T., Matsuyama, S., Tono, K., Togashi, T., Inubushi, Y., Sato, T., Tanaka, T., Kimura, T., Yokoyama, H., Kim, J., Sano, Y., Hachisu, Y., Yabashi, M., Ohashi, H., Ohmori, H., Ishikawa, T., and Yamauchi, K., "Focusing of X-ray free electron laser with reflective optics," Nature photon. 7, 43–47 (2013).

[6] Koyama, T., Yumoto, H., Senba, Y., Tono, K., Sato, T., Togashi, T., Inubushi, Y., Katayama, T., Kim, J., Matsuyama, S., Mimura, H., Yabashi, M., Yamauchi, K., Ohashi, H., and Ishikawa, T., "Investigation of ablation thresholds of optical materials using 1-μm-focusing beam at hard Xray free electron laser," Opt. Express 21, 15382 (2013).

[7] Kudo, T., Hirono, T., Nagasono, M., and Yabashi, M., "Vacuum-compatible pulse selector for free-electron laser," Rev. Sci. Instrum. 80, 093301 (2009).

[8] Tono, K., Kudo, T., Yabashi, M., Tachibana, T., Feng, Y., Fritz, D., Hastings, J., and Ishikawa, T., "Single-shot beam-position monitor for x-ray free electron laser," Rev. Sci. Instrum. 82, 023108 (2011).

[9] Bionta, R. M., "Controlling dose to low Z solids at LCLS," LCLS Technical Note No. LCLS-TN-00-3 (2000).

[10] London, R. A., Bionta, R. M., Tatchyn, R. O., and Roesler, S., "Computational simulations of high intensity x-ray matter interaction," Proc. SPIE 4500, 51–62 (2001).

[11] Yabashi, M., Higashiya, A., Tamasaku, K., Kimura, H., Kudo, T., Ohashi, H., Takahashi, S., Goto, S., and Ishikawa, T., "Optics development for Japanese XFEL project," Proc. of SPIE 6586, 658605 (2007).

[12] Kobetich, E. J., and Katz, R., "Energy Deposition by Electron Beams and δ Rays," Phys. Rev. 170, 391-396 (1968).